

A five-coordinate Mn(IV) intermediate in biological water oxidation: spectroscopic signature and a pivot mechanism for water binding

*Marius Retegan, Vera Krewald, Fikret Mamedov, Frank Neese, Wolfgang Lubitz,
Nicholas Cox* and Dimitrios A. Pantazis**

SUPPORTING INFORMATION

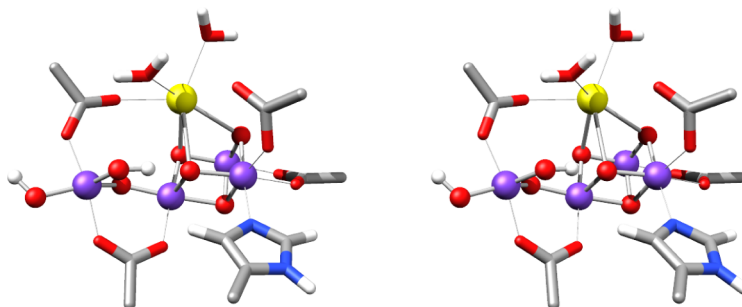


Fig. S1. Three-dimensional representation of the OEC core in the optimized S_3^B model. Selected amino acid side chains are shown for orientation.

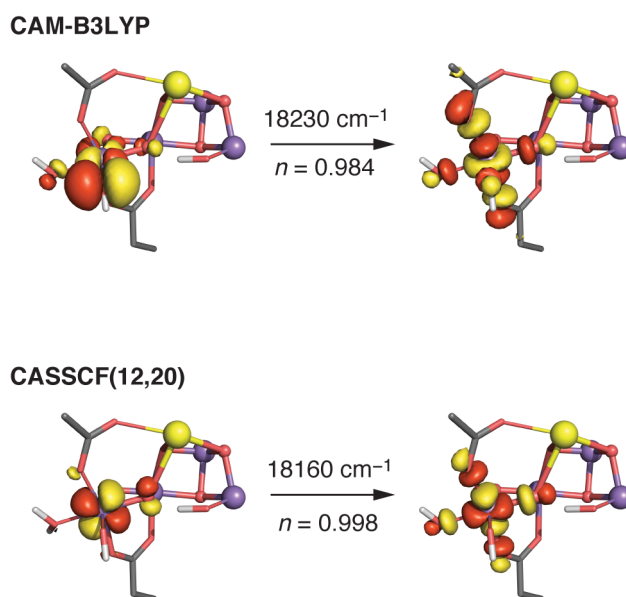


Fig. S2. Top: $S_3^{A,W}$ natural transition orbital pair for the lowest-energy transition, as obtained from CAM-B3LYP TD-DFT calculations. Bottom: CASSCF orbitals in the first excited state.

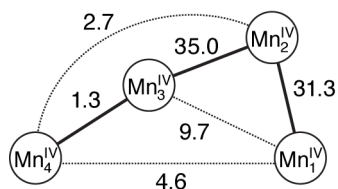


Fig. S3. Exchange coupling constants J_{ij} (cm^{-1}) for the S_3^B model.

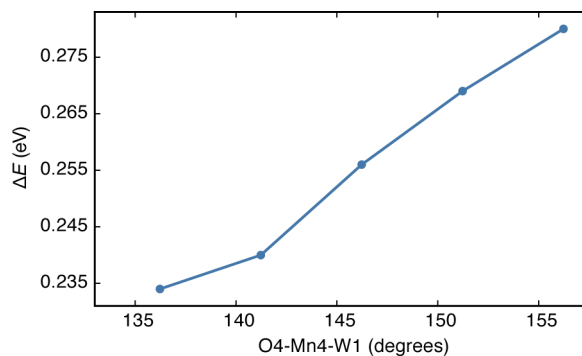


Fig. S4. Correlation between the d_{yz} - d_{z^2} orbital energy difference for the Mn4 ion of S_3^B and the O4-Mn4-W1 angle.

Table S1. Relative energies (kcal mol^{-1}) of deprotonated S_2Y_Z and $S_2Y_Z^*$ models, referenced to the lowest-energy isomer (open-cubane A-type form) for each oxidation state.

Site	$S_2^A Y_Z$	$S_2^B Y_Z$	$S_2^A Y_Z^*$	$S_2^B Y_Z^*$
W1a	0.0	15.7	0.0	14.2
W1b	16.3	29.4	16.6	27.4
W2	17.9	29.2	17.1	25.0
W3a	56.4	59.7	39.4	40.3
W3b	50.6	53.8	35.6	35.5
W4a	50.6	50.2	34.6	34.1
W4b	51.5	50.6	36.3	35.2

Table S2. Relative energies (kcal mol^{-1}) of products of water addition to S_3^B at different binding sites and various hydrogen-bonding configurations. H_a and H_b refer to the nomenclature of Figure 3 in the main text.

model	E_{rel} (kcal/mol)	W_{new} position and H-bonding
$S_3^{B,W}$ _outside-1	0.0	“outside” at Mn4, bound at the site equivalent to W1 position in S_2 H_a forms H-bond with Asp61, H_b points towards Ser169
$S_3^{B,W}$ _outside-2	3.8	“outside” at Mn4, bound at the site equivalent to W1 position in S_2 H_a forms H-bond with Asp61, H_b points towards Arg357
$S_3^{B,W}$ _inside-1	10.5	“inside” at Mn4, bound at the site <i>trans</i> to the S_2 state W1 position H-bonds with W3 and O5
$S_3^{B,W}$ _inside-2	10.7	“inside” at Mn4, bound at the site <i>trans</i> to the S_2 state W1 position H-bond only with O5
$S_3^{A,W}$ _inside-1	12.4	“inside” at Mn1, bound at the site that is empty in the S_2 state one proton forms H-bond with Glu189 carboxylate-O, the other transferred to O5 and H-bonding with $O(W_{\text{new}})$

EPR signals of trapped reduced-cluster states.

The EPR signal induced by NIR illumination arises from the OEC cluster and the Y_Z^\bullet radical. The intermediate responsible for the signal is similar, but not identical, to the transient formed during electron shuttling between the Mn cofactor and P680⁺ under physiological advancement presented above; it results instead from the one-electron oxidation of tyrosine Y_Z by the OEC cofactor, an $S_2'Y_Z^\bullet$ state.^{1, 2} Because structural relaxations are limited at the cryogenic temperatures used in experiments, S_2' designates a state of the cluster that is electronically similar to S_2 , but with a geometric structure that is similar to its parent (S_3) structure. In parallel with the formation of a signal at $g \approx 2$, characteristic of the presence of the Y_Z^\bullet radical, broadened due to the interaction with the OEC cluster, a derivative-shaped signal associated with the cluster itself is observed at $g \approx 5$. The feature was assigned to a high spin $S = 7/2$ configuration of the cluster, reminiscent of the $S = 5/2$ configuration responsible for the $g = 4.1$ signal seen in the S_2 state.³

The low-field part of the spectrum at $g \approx 5$ displays interesting similarities with the signal detected previously in samples that have undergone multiple turnovers above the S_1 state and were subsequently stored in liquid nitrogen for prolonged periods of time.⁴ Centered at $g = 5$, the signal was assigned to the same $S = 7/2$ ground state of the manganese cluster.³ To account for the subtle differences in the field position and line shape of the two signals, a more relaxed structure of the OEC cluster was assumed following incubation at 77K.

Attempts to computationally determine a structural candidate for the measured EPR signal generated by NIR illumination are hindered by the very mechanism of intramolecular electron transfer responsible for its formation, a problem that cannot be treated adequately within the present ground-state DFT approach. The comparable EPR signal measured in samples advanced

to the S_3 state and subsequently stored for extended periods of time at liquid nitrogen temperature, point towards a very similar structural configuration of the OEC cluster being formed even in the absence of the Y_Z^\bullet radical. In this case the reduced S_2'' state is generated via charge recombination of the cluster with the plastoquinone Q_A^- . This state, which contains a reduced Y_Z residue, can be approximated by one-electron reduction of the S_3^B structure.

The optimized geometrical parameters indicate that the structural differences between the parent and reduced structures are minimal. As expected, the largest differences are observed in the coordination environment of the Mn center that changes oxidation state, here the five-coordinate Mn4. We have fitted a set of six coupling constants to the energies of the different broken symmetry calculations for the reduced model. Very small differences are observed for all exchange coupling constants with the exception of J_{34} , which switches from weak ferromagnetic to antiferromagnetic. In general, J_{34} is sensitive to small structural perturbations and hence we consider it as the least well-defined parameter in the present simulations. Diagonalization of the Heisenberg Hamiltonian results in a ground state that is fourteen times degenerate, but with an extremely dense spacing of excited states at the low-energy manifold of the spin ladder. Five spin states are present below 6.5 cm^{-1} , with the remaining states appearing at significantly higher energy with respect to the ground state. The $S = 7/2$ state inferred experimentally as responsible for the $g = 5$ EPR signal, is only 5 cm^{-1} above the higher-spin ground state inferred from the calculated exchange coupling constants. Therefore, the high-spin nature of such species that contain an inorganic cluster reduced with respect to the parent S_3 structure are consistent with the parent structure being assigned as the S_3^B model.

Cartesian Coordinates

S3B							
Mn	-25.051656	-35.482828	203.983036	C	-21.721191	-33.301231	202.562857
Mn	-27.385034	-35.236831	205.423907	C	-23.059584	-33.657724	202.493310
Mn	-27.060142	-33.508890	203.297301	N	-21.292577	-33.762586	203.802220
Mn	-27.774445	-32.837195	200.198368	C	-22.317438	-34.368838	204.439124
Ca	-27.850756	-36.802494	202.344305	N	-23.408681	-34.323401	203.662027
O	-26.489108	-36.544962	204.459622	N	-21.811928	-29.565687	202.157840
O	-28.254373	-34.772967	203.904484	C	-22.904240	-28.809840	202.755200
O	-25.975989	-34.066374	204.833338	H	-22.570650	-28.449390	203.750770
O	-28.189776	-33.085634	201.949846	C	-24.174662	-29.670558	202.967461
O	-25.977044	-34.850660	202.476034	C	-24.836108	-30.135105	201.669614
O	-28.102726	-31.895575	198.706546	C	-25.833173	-31.268075	201.785254
O	-26.414112	-34.013685	199.993347	O	-25.836204	-32.015251	202.833842
O	-27.575670	-37.326782	200.026893	O	-26.574774	-31.426840	200.753908
O	-28.262579	-39.195669	202.585433	H	-25.025981	-28.877744	209.179328
H	-30.520106	-26.882433	200.170264	C	-25.296480	-29.695510	209.871270
C	-30.251370	-27.118690	201.216610	H	-25.221470	-29.303890	210.899300
H	-30.741380	-26.370660	201.865470	C	-24.358708	-30.908853	209.689655
C	-28.724639	-27.140773	201.394614	C	-24.302033	-31.412057	208.279054
C	-28.022414	-28.199020	200.517427	C	-25.104843	-32.295489	207.579119
O	-28.629400	-29.306235	200.325363	N	-23.352917	-30.981943	207.355080
O	-26.873890	-27.916906	200.036841	C	-23.547060	-31.570163	206.156931
C	-32.915980	-41.871290	196.503730	N	-24.616112	-32.366664	206.286053
C	-31.522784	-41.499776	195.963010	H	-24.695610	-37.360580	210.154300
C	-30.540419	-41.325391	197.109726	C	-25.331130	-37.102090	209.277670
C	-29.961998	-42.451565	197.735913	C	-26.310252	-38.206937	208.882370
C	-30.245984	-40.052140	197.646408	O	-26.059966	-39.035493	207.984960
C	-29.119881	-42.324483	198.853100	C	-24.383902	-36.722422	208.122859
C	-29.403097	-39.904781	198.761262	C	-25.042856	-36.084052	206.904534
C	-28.837104	-41.041653	199.370914	O	-26.268126	-35.720120	207.014452
O	-27.984686	-40.862168	200.446233	O	-24.314709	-35.947963	205.855560
H	-33.788290	-32.330730	197.916680	N	-27.496534	-38.221198	209.557851
C	-32.849000	-31.803550	197.687630	C	-28.416010	-39.351920	209.476350
C	-31.628903	-32.697334	197.555972	C	-29.294010	-39.462962	208.222336
O	-30.508457	-32.236623	197.278754	O	-29.788636	-40.555810	207.900264
H	-32.659116	-31.043868	198.466209	N	-29.521825	-38.302562	207.565103
N	-31.845655	-34.032739	197.779544	C	-30.187655	-38.240798	206.268650
C	-30.825100	-35.059340	197.615270	C	-29.450809	-37.238812	205.375540
C	-31.067523	-35.978376	196.395723	O	-29.603198	-37.246647	204.144854
O	-30.476825	-37.065305	196.293465	O	-28.717903	-36.390699	206.061146
C	-30.557084	-35.843374	198.911480	O	-25.145632	-37.693649	197.689889
C	-29.746850	-35.104225	199.978472	O	-27.125484	-35.773006	197.961163
O	-29.642472	-35.589565	201.137391	O	-26.160402	-29.908518	198.294016
O	-29.169710	-34.022085	199.562907	O	-24.344190	-31.957926	198.910999
N	-31.878983	-35.460688	195.437719	O	-29.450366	-30.485336	202.460518
C	-31.934650	-35.982310	194.075970	O	-25.786456	-39.435209	199.773165
H	-31.196480	-35.450990	193.449910	O	-27.093441	-39.097883	205.246846
H	-21.517040	-41.190080	202.040930	H	-30.307125	-30.647063	208.993297
C	-22.362150	-41.461160	202.714540	C	-31.002900	-31.050390	208.234240
C	-22.802091	-42.905624	202.588368	H	-31.846730	-31.523750	208.766240
O	-23.581647	-43.421586	203.410131	C	-30.302920	-32.075189	207.330614
C	-23.569904	-40.509526	202.481263	C	-29.095584	-31.494169	206.566351
C	-23.185797	-39.034669	202.680764	C	-28.349237	-32.544485	205.767008
C	-24.330011	-38.020527	202.694839	O	-28.157861	-33.677746	206.345321
O	-25.442954	-38.211112	202.152516	O	-27.943493	-32.231769	204.590732
O	-24.006190	-36.912781	203.311309	H	-36.667120	-31.815043	206.878892
N	-22.295440	-43.587288	201.522333	C	-36.975090	-32.284910	205.926020
C	-22.675520	-44.953280	201.229430	C	-35.746508	-32.726206	205.095106
H	-21.778710	-45.520280	200.899670	C	-34.758735	-33.621785	205.868833
C	-23.788506	-45.071323	200.162068	C	-33.696763	-34.341490	205.022188
C	-25.044057	-44.398184	200.603377	N	-32.681486	-33.438335	204.447923
C	-25.570512	-43.152495	200.309786	C	-31.698512	-33.847921	203.613423
N	-25.884878	-44.918453	201.577583	N	-31.575930	-35.154365	203.312000
C	-26.862850	-44.014617	201.845200	N	-30.857025	-32.978798	203.037814
N	-26.695577	-42.933776	201.085122	O	-27.486336	-29.373776	204.066221
H	-19.267770	-31.506790	202.779430	H	-32.851584	-42.788918	197.119050
C	-20.117520	-31.320810	202.088720	H	-33.291807	-41.069357	197.167271
C	-21.111951	-30.478354	202.870203	H	-33.691740	-42.053250	195.737530
O	-21.312802	-30.675766	204.091891	H	-31.579815	-40.565774	195.372419
C	-20.819270	-32.615451	201.578612	H	-31.163761	-42.290848	195.276012
				H	-30.174429	-43.455963	197.343139

H	-28.678056	-43.213866	199.317427	H	-28.895535	-32.172580	198.164969
H	-29.154577	-38.913396	199.161927	H	-29.247937	-29.993563	201.574937
H	-30.659850	-39.149421	197.177514	H	-28.893373	-31.292982	202.381992
H	-27.518268	-41.797881	200.778531	H	-27.147977	-30.246706	204.343995
H	-25.215235	-42.407069	199.595527	H	-28.252577	-29.655209	203.488644
H	-27.663497	-44.177997	202.568251	H	-32.944125	-35.838898	193.658047
H	-28.982513	-37.476565	207.835769	H	-31.690883	-37.056052	194.091020
H	-27.640626	-37.537408	210.299448	H	-26.573726	-40.033182	199.930734
H	-21.620947	-29.461817	201.163041	H	-25.542984	-39.130177	200.693108
H	-21.698281	-43.092146	200.862677	H	-27.921834	-39.586929	203.421370
H	-23.016802	-45.406032	202.176832	H	-27.527475	-36.719000	199.213400
H	-23.966308	-46.144006	199.955571	H	-26.338690	-36.347140	197.743892
H	-23.451229	-44.611973	199.215764	H	-26.768164	-35.051056	198.538723
H	-22.488393	-38.700471	201.885423	H	-25.193539	-38.158277	196.833129
H	-23.973590	-40.667909	201.463583	H	-25.341841	-38.397209	198.364831
H	-21.996317	-41.326613	203.750492	H	-28.183362	-39.872290	201.859718
H	-22.635135	-38.901445	203.630168	H	-26.936144	-38.055449	199.813628
H	-24.377765	-40.784790	203.184120	H	-24.963643	-32.647592	199.230490
H	-26.346747	-29.974157	209.675386	H	-24.951631	-31.180916	198.726726
H	-25.970926	-32.882106	207.887936	H	-26.935219	-30.511682	198.425479
H	-22.919316	-31.410520	205.270411	H	-26.364869	-29.192712	198.976543
H	-23.782529	-33.501368	201.692865	H	-26.889313	-39.227607	206.200895
H	-22.254845	-34.846837	205.415958	H	-26.706973	-38.206928	205.046077
H	-19.710351	-30.778196	201.217368	H	-25.767041	-45.813502	202.049984
H	-23.111815	-27.935750	202.115621	H	-22.597365	-30.324384	207.551999
H	-29.892390	-34.519088	197.358478				
H	-32.779352	-34.330817	198.062050				
H	-32.965436	-31.263928	196.731334	TS model for water binding			
H	-32.245714	-34.523531	195.598290	Mn	-25.018257	-35.493159	204.009609
H	-30.685327	-28.106687	201.449483	Mn	-27.376119	-35.247249	205.414554
H	-20.048445	-33.325990	201.223630	Mn	-27.035899	-33.537749	203.261686
H	-21.439624	-32.363333	200.699897	Mn	-27.543405	-32.965055	200.126004
H	-25.908190	-36.212140	209.591630	Ca	-27.762231	-36.873173	202.335097
H	-30.086476	-39.229271	205.784754	O	-26.445829	-36.560543	204.481760
C	-31.678626	-37.868496	206.377944	O	-28.214020	-34.802987	203.876295
H	-32.145353	-37.863505	205.377097	O	-25.964158	-34.073990	204.826418
H	-32.202570	-38.615775	206.997047	O	-28.051687	-33.155718	201.837839
H	-31.800294	-36.876115	206.848309	O	-25.920963	-34.897530	202.487293
H	-29.091856	-39.304672	210.347804	O	-27.549839	-32.116504	198.465625
H	-27.846440	-40.296220	209.551350	O	-26.235376	-34.182284	199.985977
H	-23.613141	-36.014032	208.481742	O	-27.404149	-37.476699	200.027074
H	-23.838112	-37.610833	207.757739	O	-28.150216	-39.265219	202.636088
H	-29.950953	-36.734203	198.653656	C	-32.915382	-41.867907	196.503232
H	-31.488213	-36.222675	199.370316	C	-31.686972	-41.037900	196.080090
H	-31.398227	-30.196402	207.653728	C	-30.661732	-40.951518	197.199418
H	-29.958586	-32.934809	207.933844	C	-29.867574	-42.075315	197.521040
H	-28.363907	-31.070851	207.285658	C	-30.502329	-39.793586	197.992813
H	-31.021873	-32.490115	206.595919	C	-28.957151	-42.056214	198.588970
H	-29.376614	-30.673667	205.883172	C	-29.594164	-39.752155	199.066251
H	-28.277260	-26.153187	201.180442	C	-28.821833	-40.889961	199.374059
H	-28.461858	-27.383788	202.444485	O	-27.919748	-40.828409	200.419369
H	-24.687533	-31.739831	210.339243	H	-31.749553	-34.524043	197.899322
H	-23.333638	-30.647745	210.012151	C	-30.824951	-35.055921	197.615397
H	-25.064051	-32.997701	205.560006	H	-31.031953	-35.694479	196.734973
H	-37.552410	-31.538150	205.353920	C	-30.275100	-35.898264	198.770632
H	-35.218514	-31.827190	204.718502	C	-29.484596	-35.158314	199.841205
H	-35.324314	-34.422399	206.383610	O	-29.323779	-35.652208	200.973166
H	-33.184180	-35.085874	205.664414	O	-28.941993	-34.037615	199.423124
H	-37.631483	-33.141729	206.162816	H	-21.615410	-41.195356	201.941962
H	-36.094324	-33.271421	204.194711	C	-22.362233	-41.457632	202.715189
H	-34.261764	-33.042443	206.673546	C	-22.803503	-42.901324	202.588257
H	-32.742926	-32.442551	204.650222	O	-23.558074	-43.430227	203.425733
H	-34.189347	-34.894373	204.197608	C	-23.582110	-40.508257	202.618635
H	-30.941408	-31.961771	203.108811	C	-23.149976	-39.033281	202.635857
H	-31.969413	-35.876583	203.906526	C	-24.281972	-38.013785	202.716687
H	-29.978981	-33.310409	202.606305	O	-25.396855	-38.185260	202.168838
H	-30.826404	-35.443373	202.672551	O	-23.954870	-36.936690	203.377118
H	-23.892429	-30.552203	203.567614	N	-22.322924	-43.572251	201.503953
H	-25.355059	-29.312088	201.141073	C	-22.675275	-44.949679	201.229839
H	-24.908221	-29.097572	203.564260	H	-21.775854	-45.485650	200.875916
H	-24.092520	-30.536963	200.946649	C	-23.803043	-45.107656	200.182868
H	-20.365880	-33.615068	204.199919	C	-25.064148	-44.433289	200.605461
H	-26.109986	-34.416117	200.869144	C	-25.611151	-43.213321	200.249446
				N	-25.902583	-44.921912	201.597947

C	-26.900530	-44.025760	201.814386	H	-25.259868	-42.493167	199.507905
N	-26.748037	-42.980511	201.003283	H	-27.701713	-44.167874	202.541268
H	-19.304547	-31.605586	202.778049	H	-28.891269	-37.569417	207.726734
C	-20.118029	-31.317136	202.090207	H	-27.677480	-37.486676	210.209408
C	-21.140983	-30.516393	202.885247	H	-21.531378	-29.390959	201.218245
O	-21.395370	-30.768300	204.083779	H	-21.742637	-43.071937	200.833530
C	-20.831029	-32.587982	201.518374	H	-22.982828	-45.405692	202.186893
C	-21.704655	-33.318134	202.501391	H	-23.971609	-46.187893	200.010289
C	-23.039969	-33.692220	202.458277	H	-23.479419	-44.675071	199.219214
N	-21.250831	-33.769913	203.735927	H	-22.580440	-38.789843	201.715129
C	-22.262631	-34.373517	204.397680	H	-24.143125	-40.730341	201.691995
N	-23.366993	-34.343145	203.641106	H	-21.872324	-41.339145	203.700087
N	-21.790395	-29.553618	202.189251	H	-22.464908	-38.835008	203.479040
C	-22.904942	-28.806341	202.756540	H	-24.269746	-40.712894	203.459573
H	-22.590077	-28.384738	203.728961	H	-26.353471	-29.909263	209.632637
C	-24.158508	-29.675086	202.954786	H	-26.028254	-32.922829	207.919249
C	-24.613061	-30.293890	201.638142	H	-22.926420	-31.509663	205.336964
C	-25.665713	-31.374858	201.728571	H	-23.779300	-33.567794	201.667637
O	-25.756355	-32.068569	202.796271	H	-22.181236	-34.837761	205.380091
O	-26.339745	-31.528272	200.646376	H	-19.676483	-30.741550	201.259135
H	-24.950067	-28.888474	209.199228	H	-23.116745	-27.962068	202.078636
C	-25.297896	-29.692548	209.872303	H	-30.083055	-34.303902	197.298080
H	-25.238898	-29.316732	210.908430	H	-20.063668	-33.275314	201.113638
C	-24.423734	-30.957561	209.730405	H	-21.470900	-32.297720	200.666221
C	-24.345805	-31.472990	208.327052	H	-25.894789	-36.223119	209.646328
C	-25.148708	-32.350871	207.620951	H	-29.815299	-39.337295	205.669046
N	-23.377791	-31.059193	207.415521	C	-31.601028	-38.224458	206.206855
C	-23.564168	-31.653603	206.218034	H	-32.007973	-38.234837	205.181382
N	-24.642857	-32.436418	206.337014	H	-32.037443	-39.064693	206.772111
H	-24.732989	-37.477093	210.129019	H	-31.884374	-37.276551	206.697066
C	-25.332123	-37.099094	209.278261	H	-29.073121	-39.293865	210.362184
C	-26.293403	-38.219160	208.880524	H	-27.844428	-40.291679	209.549854
O	-25.999685	-39.086055	208.034048	H	-23.610703	-35.992445	208.521714
C	-24.373546	-36.700137	208.145340	H	-23.819649	-37.582300	207.777006
C	-25.026584	-36.056983	206.926712	H	-29.533691	-36.629909	198.387256
O	-26.255836	-35.708461	207.024810	H	-31.056021	-36.492134	199.277596
O	-24.285976	-35.909785	205.886336	H	-31.506561	-30.314321	207.576822
N	-27.500650	-38.215074	209.519373	H	-29.782155	-32.847592	208.097693
C	-28.416915	-39.349086	209.476480	H	-28.379465	-30.982636	207.133847
C	-29.313960	-39.503755	208.240702	H	-30.947733	-32.669357	206.781254
O	-29.860774	-40.591888	207.993533	H	-29.538581	-30.766765	205.809023
N	-29.459507	-38.388270	207.494940	H	-24.823267	-31.763948	210.371077
C	-30.070521	-38.383575	206.170038	H	-23.398520	-30.751568	210.090819
C	-29.401157	-37.293335	205.326068	H	-25.096323	-33.063643	205.600919
O	-29.543889	-37.272074	204.097194	H	-23.938816	-30.476027	203.678895
O	-28.697234	-36.432141	206.036508	H	-24.963429	-29.532824	200.918528
O	-24.784249	-37.851907	197.850863	H	-24.962928	-29.055083	203.391057
O	-26.801062	-35.951331	197.946495	H	-23.755129	-30.799841	201.145567
O	-25.583364	-39.583880	199.862779	H	-20.322358	-33.605914	204.122237
O	-26.922811	-39.141317	205.246450	H	-26.006889	-34.560918	200.899138
H	-30.324525	-30.487784	208.904524	H	-28.085509	-32.634633	197.828552
C	-31.004076	-31.047608	208.234585	H	-26.417236	-40.125811	199.972182
H	-31.776701	-31.528535	208.860328	H	-25.431982	-39.203299	200.776408
C	-30.239387	-32.105202	207.418057	H	-27.772702	-39.642400	203.462926
C	-29.135359	-31.512626	206.516672	H	-27.314906	-36.878860	199.217187
C	-28.369982	-32.556068	205.714192	H	-25.987994	-36.516971	197.825370
O	-28.156855	-33.682850	206.307943	H	-26.512436	-35.217661	198.550093
O	-27.972888	-32.245446	204.536488	H	-24.773107	-38.322455	196.996090
H	-32.598812	-42.866724	196.858474	H	-25.051781	-38.547122	198.512396
H	-33.441284	-41.378260	197.344128	H	-28.062998	-39.930160	201.901942
H	-33.652078	-42.032949	195.695389	H	-26.786422	-38.221525	199.827094
H	-32.002217	-40.020786	195.779377	H	-26.742050	-39.261650	206.206228
H	-31.219765	-41.499455	195.187815	H	-26.600932	-38.221681	205.058027
H	-29.961369	-42.990827	196.920272	H	-25.772291	-45.791105	202.113448
H	-28.345794	-42.939041	198.811392	H	-22.615309	-30.412855	207.621313
H	-29.451852	-38.840027	199.658543	O	-28.981189	-30.166712	199.822721
H	-31.100710	-38.899625	197.767773	H	-28.237194	-29.810162	200.343242
H	-27.514641	-41.811742	200.703047	H	-28.516500	-30.693443	199.121816

REFERENCES

1. N. Ioannidis and V. Petrouleas, *Biochemistry*, 2000, **39**, 5246-5254.
2. A. Boussac, M. Sugiura, Y. Inoue and A. W. Rutherford, *Biochemistry*, 2000, **39**, 13788-13799.
3. Y. Sanakis, N. Ioannidis, G. Sioros and V. Petrouleas, *J. Am. Chem. Soc.*, 2001, **123**, 10766-10767.
4. J. H. A. Nugent, S. Turconi and M. C. W. Evans, *Biochemistry*, 1997, **36**, 7086-7096.